JOURNAL OF MAGNETIC RESONANCE **130,** 68–75 (1998)
ARTICLE NO. MN971277

Two-Dimensional NMR Experiments for the Assignment of Aromatic Side Chains in ^{13}C-labeled Proteins

Jeanine J. Prompers,* Anneke Groenewegen,† Cornelis W. Hilbers,* and Henri A. M. Pepermans†,[1]

*Nijmegen SON Research Center, Laboratory of Biophysical Chemistry, University of Nijmegen, Toernooiveld, 6525 ED Nijmegen, The Netherlands; and †Unilever Research Laboratory, Olivier van Noortlaan 120, 3133 AT Vlaardingen, The Netherlands

Received March 25, 1997; revised July 10, 1997

As aromatic residues very often are part of the hydrophobic core of proteins, the unambiguous assignment of the aromatic proton resonances is essential for an accurate and precise structure determination. Instead of transferring $^1H^\beta$ coherence to the aromatic protons via $^{13}C^\gamma$ like in a number of published methods, in our new experiments the $^{13}C^\gamma$ resonances are first correlated with the $^1H^\beta$ chemical shifts in one experiment and then with the aromatic proton resonances in four other experiments. Their short coherence transfer pathways make the experiments applicable to proteins with a molecular weight larger than 20 kDa, as is demonstrated for *Fusarium solani pisi* cutinase (214 residues). The dispersion of the C^γ chemical shifts between different aromatic residue types is obvious, but even the dispersion within one type is sufficient to combine the experiments using only the C^γ chemical shift and to assign nearly all aromatic proton resonances of cutinase.

Key Words: **heteronuclear NMR; resonance assignment; aromatic side chain; protein; cutinase.**

Complete resonance assignments are essential for accurate structure determination by NMR. A whole suite of 3D triple-resonance experiments has been developed in the past seven years which allows the assignment of the backbone and aliphatic side-chain resonances of ^{13}C, ^{15}N-labeled proteins (*1, 2*). In this approach connectivities are established via the scalar coupling network and are thus free of the ambiguities encountered in assignment strategies based on through-space interactions (*3*). In contrast, the assignment of aromatic ^{1}H and ^{13}C resonances usually relies on NOE connectivities from the previously assigned aliphatic part to the ring protons. Because of the high density of NOEs involving aromatic protons and the poor dispersion of aromatic chemical shifts (*4*), it may be difficult to obtain complete, unambiguous assignments of aromatic resonances for larger proteins. In many proteins the aromatic residues are part of a hydrophobic core. Unambiguous assignment of the NOEs resulting from the close side-chain contacts in such a core is essential for an accurate and precise structure determination. Therefore, methods for the unambiguous assignment of aromatic ring protons are highly desirable. The reverse labeling technique introduced by Vuister *et al.* (*5*) facilitates the assignment process, but requires an (expensive) additional sample. The conventional HCCH–COSY (*6, 7*) and the three-dimensional ^{1}H-TOCSY-relayed ct-[^{13}C,^{1}H]-HMQC (*8*) experiments correlate carbons and protons within the aromatic ring, but they do not establish the connection with the aliphatic carbons and protons. An HCCH–TOCSY (*9, 10*) experiment optimized for the aromatic resonances is not suited for transferring coherence between the β- and γ-carbon spins of aromatic residues, because of the large chemical shift differences between these nuclei. Several experiments have been proposed to achieve transfer between $^{13}C^\beta$ and $^{13}C^\gamma$ atoms, among which are the polarization-transfer-based experiments proposed by Yamazaki *et al.* (*11*), the AMNESIA sequence proposed by Grzesiek and Bax (*12*), and the PLUSH TACSY experiment recently proposed by Carlomagno *et al.* (*13*). Löhr and Rüterjans (*14*) introduced additional experiments [HCBCG, H(CD)CGCB, and (HC)C–(C)CH–TOCSY] which, in combination, provide assignments in the presence of partial chemical shift degeneracy. In all these experiments, the aromatic proton resonances are linked to the aliphatic portion of the residue by transferring $^1H^\beta$ coherence to the aromatic protons (*11–14*) or by transferring $^1H^\delta$ coherence to $^{13}C^\beta$ in an out-and-back manner (*14*). For larger proteins, these methods become increasingly less sensitive due to relaxation during the multiple transfer steps. In this article, we present five straightforward [^{13}C, ^{1}H] correlation experiments for making aromatic resonance assignments.

In the five new pulse sequences $^{13}C^\gamma$ resonances are correlated with $^1H^\beta$ [CG(CB)H], with $^1H^\delta$ [CG(CD)H], with $^1H^\epsilon$ [CG(CDCE)H], with $^1H^\zeta$ [CG(CDCECZ)H], or with all aromatic proton resonances [CG(C^{aro})H–TOCSY]. In principle, the coherence transfer pathway of the experiments mentioned above (*11–14*) is divided into two pieces. Instead of transferring $^1H^\beta$ coherence to the aromatic protons via $^{13}C^\gamma$, the $^{13}C^\gamma$ resonances are first correlated with the $^1H^\beta$

[1] To whom correspondence should be addressed. Fax: 31-104605383. E-mail: Rik.Pepermans@Unilever.com.

1090-7807/98 $25.00

chemical shifts in one experiment and then with the aromatic proton resonances in four separate experiments. The method relies on the dispersion of the $^{13}C^{\gamma}$ chemical shifts. Phenylalanines and tyrosines have very different $^{13}C^{\gamma}$ chemical shifts, excluding mutual overlap, hence making it possible to distinguish the two amino-acid types. Phenylalanine and tyrosine $^{13}C^{\gamma}$ resonances from the BioMagResBank (*15*) show that also within one amino-acid type the $^{13}C^{\gamma}$ chemical shift can differ by 5 ppm.

Whereas the HCBCG experiment proposed by Löhr and Rüterjans (*14*) is similar to the HCACO (*16*), the CG(CB)H introduced here resembles the COCAH experiment (*17*). The HCBCG experiment is of the out-and-back type, starting with magnetization from $^{1}H^{\beta}$. In the CG(CB)H experiment coherence originating from $^{13}C^{\gamma}$ is transferred one way. Figure 1A illustrates the pulse sequence that has been developed to provide $^{13}C^{\gamma}$ to $^{1}H^{\beta}$ correlations. The building blocks used to transfer coherence from $^{13}C^{\gamma}$ (t_1) $\rightarrow$ $^{13}C^{\beta}$ $\rightarrow$ $^{1}H^{\beta}$ (t_2) have been described in Dijkstra *et al.* (*17*). Below we will focus on a number of important features in the pulse scheme.

The evolution of $^{13}C^{\gamma}$ is recorded in a constant-time manner. The constant-time period is chosen to be $1/^{1}J_{C\gamma C\delta}$, so that dephasing due to both $^{13}C^{\delta}$'s is refocused (*18*). In the meantime, $^{13}C^{\gamma}$ defocuses with respect to $^{13}C^{\beta}$ during $1/2^{1}J_{C\gamma C\beta}$, so that $^{13}C^{\gamma}$ is antiphase with respect to $^{13}C^{\beta}$ after the constant-time evolution period. The 180° $^{13}C^{\beta}$ pulse is compensated for its Bloch–Siegert effect (*19*). After the constant-time evolution period, antiphase $^{13}C^{\gamma}$ coherence is converted into antiphase $^{13}C^{\beta}$ coherence. This antiphase $^{13}C^{\beta}$ coherence is refocused with respect to $^{13}C^{\gamma}$, and in the meantime it is defocused with respect to its bound $^{1}H^{\beta}$'s during $1/4^{1}J_{C\beta H\beta}$. The passive $^{1}J_{C\alpha C\beta}$ coupling that would otherwise lead to a major loss of detectable magnetization has been removed as described by Yamazaki *et al.* (*11*). After converting antiphase $^{13}C^{\beta}$ coherence into antiphase $^{1}H^{\beta}$ coherence, a final reverse INEPT yields observable $^{1}H^{\beta}$ magnetization. Gradients are used in this sequence to suppress artifacts and to aid in the removal of water (*20*).

The CG(CD)H, CG(CDCE)H, and CG(CDCECZ)H experiments are variations on the CG(CB)H. The pulse sequences are illustrated in Figs. 1B and 1C. Again the $^{13}C^{\gamma}$ chemical shift is recorded in a constant-time evolution period, which is now tuned to $3/4^{1}J_{C\gamma C\delta}$, which was selected among the possible $(2n + 1)/4^{1}J_{C\gamma C\delta}$ durations as a compromise between relaxation losses and the need to record a sufficient number of t_1 points. After this period $^{13}C^{\gamma}$ is antiphase with respect to $^{13}C^{\delta}$. The passive coupling of $^{13}C^{\gamma}$ to $^{13}C^{\beta}$ is eliminated by a 180° pulse on $^{13}C^{\beta}$. To start selectively from $^{13}C^{\gamma}$, all aromatic carbons with a bound proton are dephased during $1/2^{1}J_{CH}$ (*21*). Thus, $^{13}C^{\delta}$, $^{13}C^{\epsilon}$, and Phe-$^{13}C^{\zeta}$ coherences will be antiphase with respect to their attached proton after the constant-time period. These unwanted coherences are purged by the subsequent pair of orthogonal ^{1}H spin-lock pulses (*22*). The homonuclear COSY pulse converts antiphase $^{13}C^{\gamma}$ coherence into antiphase $^{13}C^{\delta}$ coherence. In the CG(CD)H experiment, $^{13}C^{\delta}$ is rephased with respect to $^{13}C^{\gamma}$ during $1/4^{1}J_{C\gamma C\delta}$ and dephased with respect to $^{1}H^{\delta}$ during $1/2^{1}J_{C\delta H\delta}$. Antiphase $^{13}C^{\delta}$ coherence is subsequently converted into antiphase $^{1}H^{\delta}$ coherence, which is converted into observable magnetization by a reverse INEPT. In the CG(CDCE)H experiment, the antiphase $^{13}C^{\delta}$ coherence created after the constant-time $^{13}C^{\gamma}$ evolution period is rephased with respect to $^{13}C^{\gamma}$ and in the meantime dephased with respect to $^{13}C^{\epsilon}$ during $1/2^{1}J_{CC}$. Protons are decoupled during this period. Just before the subsequent $^{13}C^{aro}$ pulse, which converts antiphase $^{13}C^{\delta}$ coherence into antiphase $^{13}C^{\epsilon}$ coherence, a pair of orthogonal ^{1}H spin-lock pulses (*22*) is applied. Antiphase $^{13}C^{\epsilon}$ coherence is converted into observable $^{1}H^{\epsilon}$ magnetization in a manner analogous to the CG(CD)H experiment. Likewise, in phenylalanines the coherence can be relayed even further to the ζ carbon and proton in a CG(CDCECZ)H experiment.

We furthermore present a TOCSY version [CG(C^{aro})H–TOCSY] of the experiments discussed in the previous paragraph. The pulse sequence is given in Fig. 1D. The strong coupling between the aromatic carbons, which is detrimental for relay-type transfer experiments, makes it particularly attractive to use a TOCSY transfer (*12*). Also in the CG(C^{aro})H–TOCSY experiment, signals originating from aromatic carbons with a bound proton are eliminated. Here, antiphase $^{13}C^{\delta}$, $^{13}C^{\epsilon}$, and Phe-$^{13}C^{\zeta}$ coherences, created during the constant-time $^{13}C^{\gamma}$ evolution period, are destroyed by a 90° ^{1}H pulse followed by a gradient. At the time of the gradient, the desired magnetization is of the form $^{13}C_z^{\gamma}$, as the constant-time period is tuned to $1/^{1}J_{C\gamma C\delta}$, so that dephasing due to both $^{13}C^{\delta}$'s is refocused (*18*). After the mixing period, a reverse refocused INEPT converts the aromatic carbon magnetization into aromatic proton magnetization, which is detected. A pair of orthogonal ^{1}H spin-lock pulses (*22*) is applied after the mixing period for water suppression and a ^{13}C spin-lock pulse is applied after the first carbon pulse following the mixing period in order to remove artifacts.

The experiments described in this article were recorded on a 2 mM sample of ^{13}C, ^{15}N-labeled *Fusarium solani pisi* cutinase (214 amino acids) in 95%/5% H_2O/D_2O, 10 mM deuterated sodium acetate, 100 mM NaCl, 0.02% sodium azide at pH 5.0 and 25°C (*28*). Under these conditions, cutinase is a monomeric protein with a rotational correlation time of about 11 ns, as determined from ^{15}N relaxation studies (to be published). The experiments were performed on a Bruker 600 MHz AMX spectrometer equipped with a Bruker BLAX 300-W linear amplifier and a 5-mm inverse triple-resonance probehead ($^{1}H/^{15}N/^{13}C$) with a self-shielded *z*-gradient coil. The spectral widths were 2415 Hz (ω_1) and 7246 Hz (ω_2). The CG(CB)H was collected with 38 complex points in t_1; the CG(CD)H, CG(CDCE)H, and

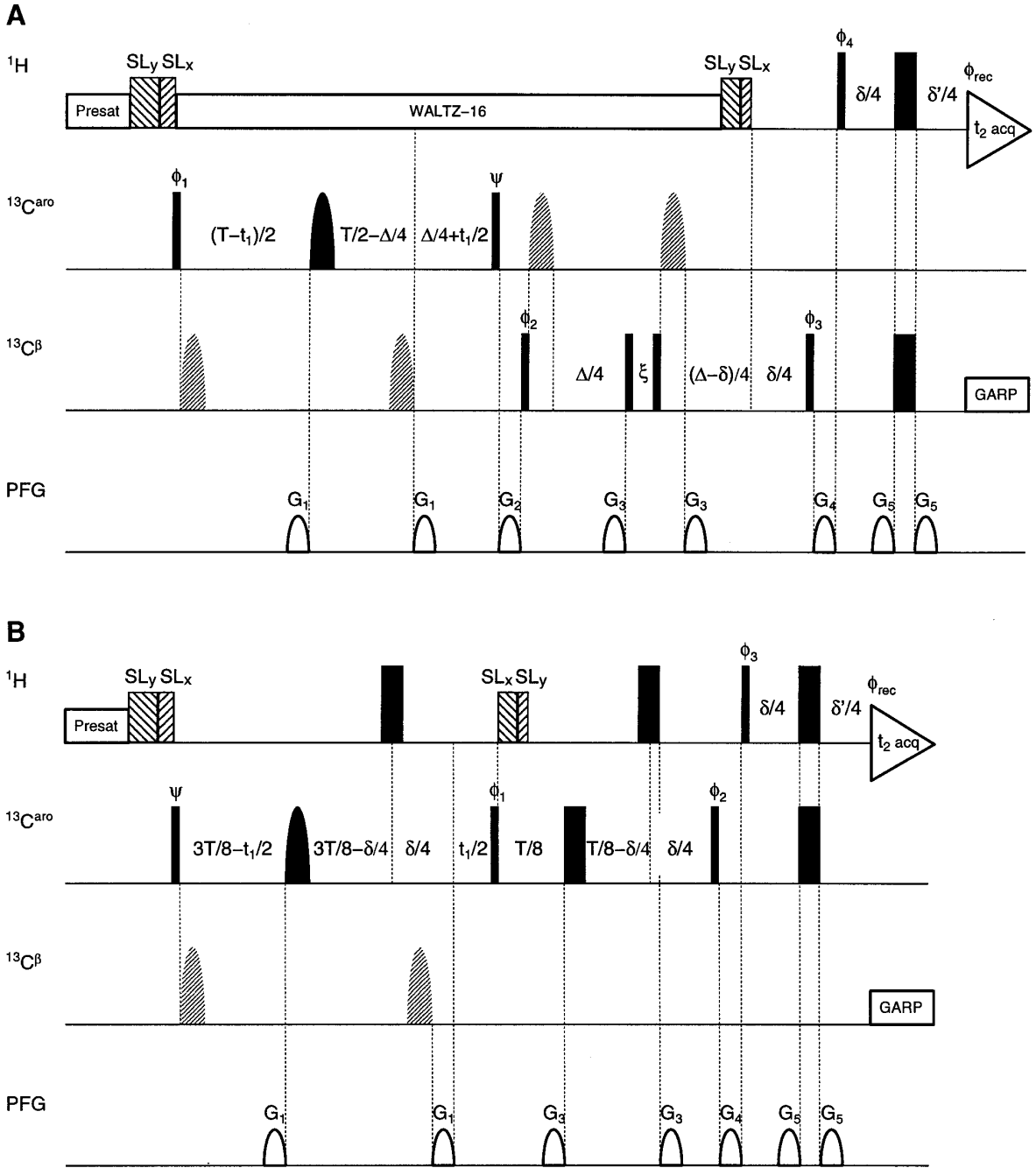

FIG. 1. Pulse schemes for the (A) CG(CB)H, (B) CG(CD)H, (C) CG(CDCE)H, and (D) CG(C^{aro})H-TOCSY experiments. All narrow (wide) pulses have a flip angle of 90° (180°). Pulses for which the phases are not indicated are applied along the *x* axis. All carbon pulses are generated using a single synthesizer. For the CG(CB)H experiment the carbon frequency jumps from 134 to 40 ppm immediately after the pulse with phase ψ. In the CG(CD)H, CG(CDCE)H, and CG(C^{aro})H-TOCSY experiments the carbon carrier is maintained at 134 ppm. Unless stated otherwise, carbon 90° and rectangular 180° pulses are applied with a 3.5-kHz field, so that application of $^{13}C^{\beta}$ pulses introduces minimal perturbations of $^{13}C^{\gamma}$ spins and vice versa (*23*). The pulses after the pulse with phase ϕ_1 in the CG(CDCE)H experiment and the pulses after the mixing period in the CG(C^{aro})H–TOCSY experiment are applied with a 22.7-kHz field. The shaped $^{13}C^{\beta}$ and $^{13}C^{aro}$ (aromatic) pulses are 180° pulses with an amplitude profile corresponding to the central lobe of a sinc function of durations 140 and 105 μs, respectively. Hatched pulses are applied off-resonance. Water suppression is achieved by rather intense ($\gamma B_1 \approx 175$ Hz) presaturation of the water signal, followed by a pair of orthogonal 26.3-kHz ^{1}H spin-lock pulses (*22*) of 4 and 2 ms, respectively. The other pairs of ^{1}H spin-lock pulses have durations of 400 and 200 μs, respectively, and are applied for additional water suppression and for the removal of unwanted signals. ^{1}H and ^{13}C decoupling are achieved using 4.7-kHz WALTZ-16 (*24*) and 3.3-kHz GARP (*25*) decoupling fields, respectively. In the TOCSY experiment a 7.1-kHz FLOPSY-8 (*26*) spin-lock sequence is used. Spectra were recorded with mixing periods of 3.3, 6.6, and 13.2 ms. The ^{13}C spin-lock pulse after the mixing period is applied at 22.7 kHz and has a duration of 1 ms. The delays used are: (A) $T = 1/^1J_{C\gamma C\delta} = 16.7$ ms, $\Delta = 1/^1J_{C\gamma C\beta} = 20.0$ ms, $\delta = 1/^1J_{C\beta H\beta} = 7.1$ ms, $\xi = [(2\Delta_f)^{-1} - (4/\pi)\tau_{90°}] = 108.6$ μs (Δ_f is the typical difference between the

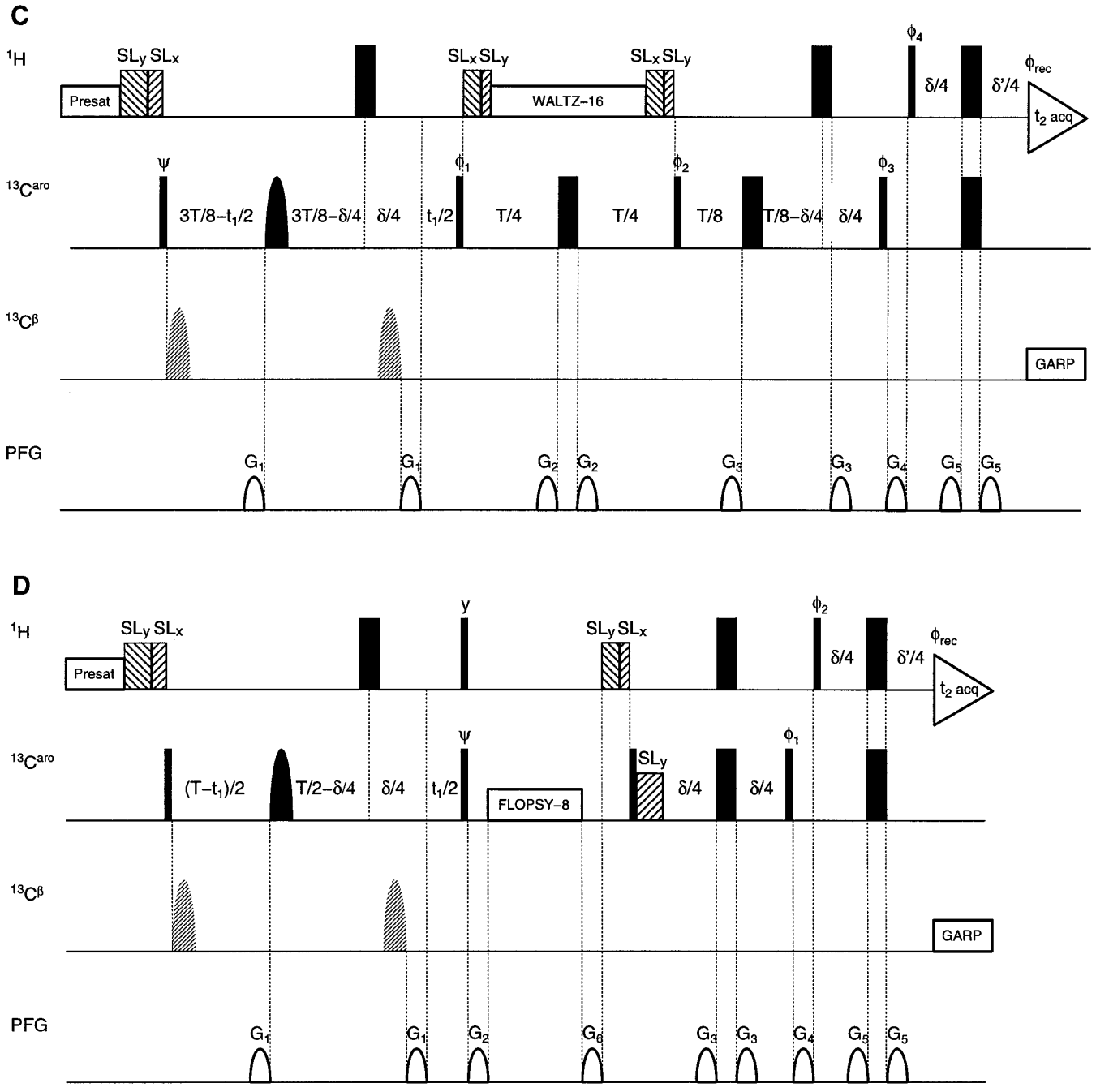

FIG. 1—*Continued*

resonance frequencies of $^{13}C^{\alpha}$ and $^{13}C^{\beta}$ in aromatic amino-acid residues, which is about 2.5 kHz; $\tau_{90°}$ is the duration of the 90° $^{13}C^{\beta}$ pulses); (B–D) $T = 1/^1J_{CC} = 16.7$ ms, $\delta = 1/^1J_{CH} = 6.25$ ms (for aromatic carbons and protons). The delay δ' was adjusted empirically in comparison to δ to refocus ^{1}H exactly at the first sampling point of the acquisition in order to give a 0° linear phase correction in the acquisition dimension. Spectra were recorded with prescan recovery delays of 1.5 s. The phase cycling employed is: (A) $\phi_1 = 16(x), 16(-x); \psi = y, -y; \phi_2 = 8(y), 8(-y); \phi_3 = 2(y), 2(-y); \phi_4 = 4(x), 4(-x); \phi_{rec} = x, 2(-x), x, -x, 2(x), 2(-x), 2(x), -x, x, 2(-x), x, -x, 2(x), -x, x, 2(-x), 2(x), 2(-x), x, -x, 2(x), -x$; (B) $\psi = 8(x), 8(-x); \phi_1 = 2(y), 2(-y); \phi_2 = y, -y; \phi_3 = 4(x), 4(-x); \phi_{rec} = 2(x, -x), 4(-x, x), 2(x, -x)$; (C) $\psi = 16(x), 16(-x); \phi_1 = 2(y), 2(-y); \phi_2 = 4(y), 4(-y); \phi_3 = y, -y; \phi_4 = 8(x), 8(-x); \phi_{rec} = 4(x, -x), 8(-x, x), 4(x, -x)$; (D) $\psi = 4(x), 4(-x); \phi_1 = 2(y), 2(-y); \phi_2 = x, -x; \phi_{rec} = x, 2(-x), x, -x, 2(x), -x$. Quadrature detection in t_1 is obtained by States–TPPI (*27*) of ψ. The duration of the gradients is 100 μs, and the strengths are as follows: $G_1 = 13.0$ G/cm, $G_2 = 11.5$ G/cm, $G_3 = 8.5$ G/cm, $G_4 = 3.5$ G/cm, $G_5 = 2.5$ G/cm, $G_6 = 26.5$ G/cm.

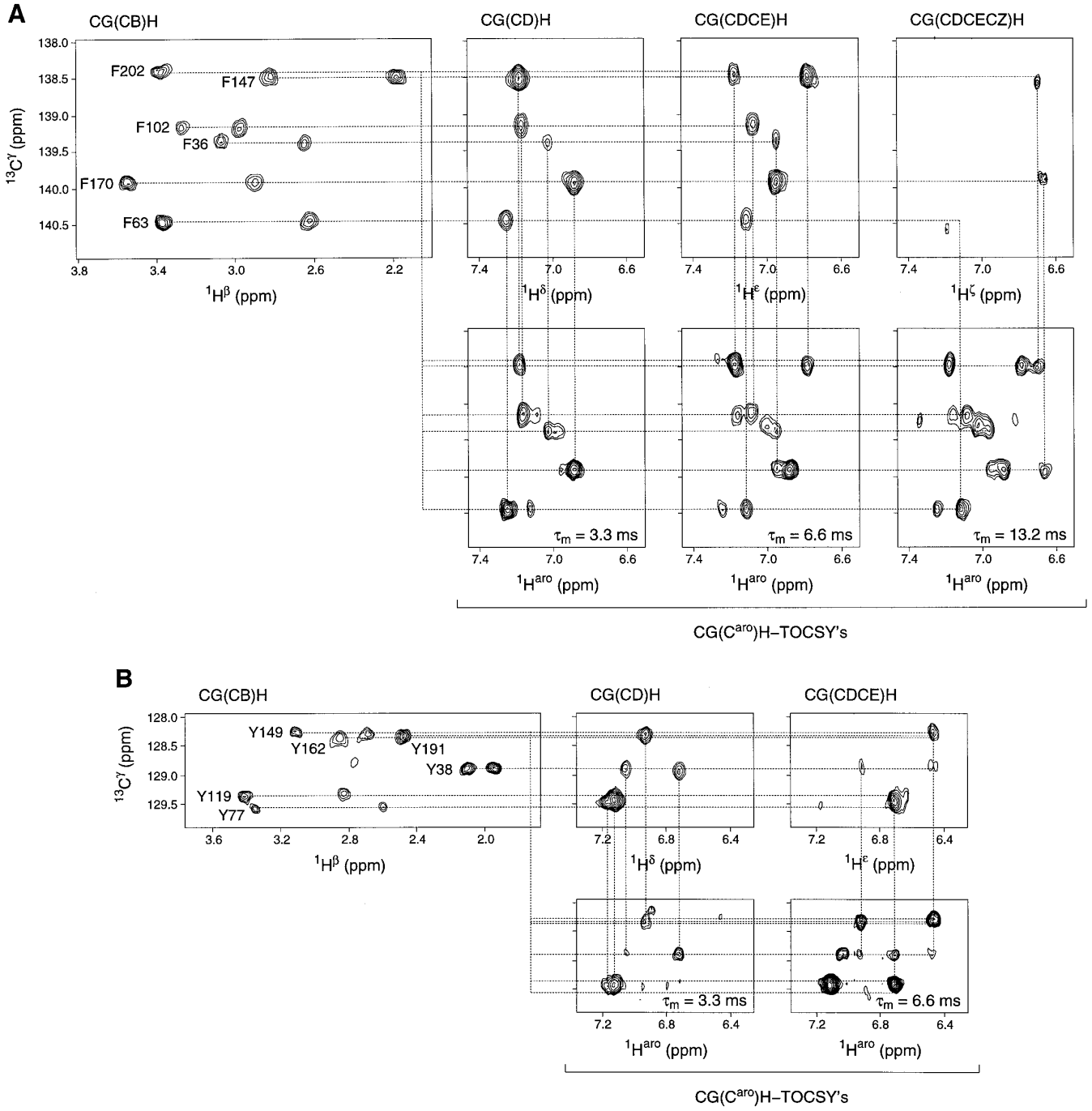

FIG. 2. Assignment of all $^{13}C^{\gamma}$ and aromatic ^{1}H resonances of the (A) phenylalanine and (B) tyrosine residues of *F. solani pisi* cutinase by combining the CG(CB)H, CG(CD)H, CG(CDCE)H, CG(CDCECZ)H, and CG(C^{aro})H-TOCSY experiments. The lowest plot levels for the CG(CB)H and CG(CD)H spectra are two and five times higher, respectively, than for the other spectra. Dotted lines indicate common chemical shifts of the correlations in the individual spectra.

CG(CDCECZ)H were collected with 27 complex points in t_1; the CG(C^{aro})H–TOCSY was collected with 37 complex points in t_1; and all were collected with 512 complex points in t_2. For the CG(CB)H and CG(C^{aro})H–TOCSY experiments 1216 scans were collected for each FID, whereas the others were recorded with 1600 scans, resulting in total acquisition times ranging from 40 to 43 h. All spectra were apodized in t_1 and t_2 using a squared-cosine-bell. The t_1 data points were mirror imaged and subsequently doubled by linear prediction (*29*), which resulted in three times the

points originally acquired, after removing the mirror-imaged points. Additional zero-filling yielded final spectrum sizes of $256(\omega_1) \times 1024(\omega_2)$.

Figure 2 shows the spectra obtained. The $^1H^\beta$, $^{13}C^\gamma$ signals of all six phenylalanines are nicely resolved. Only Phe^{147} and Phe^{202} have nearly degenerate $^{13}C^\gamma$ chemical shifts. All $^1H^\delta$'s and $^1H^\epsilon$'s, as well as three out of the six $^1H^\zeta$'s could be assigned. Three out of the six tyrosines of cutinase have nearly overlapping $^{13}C^\gamma$, $^1H^\delta$, and $^1H^\epsilon$ chemical shifts: Tyr^{149}, Tyr^{162}, and Tyr^{191}. The $^1H^\delta$ and $^1H^\epsilon$ chemical shifts of the remaining three tyrosines could be assigned. For Tyr^{38} two $^1H^\delta$ and two $^1H^\epsilon$ signals are observed, implying that its aromatic ring flips slowly on the NMR time scale defined by the chemical shift differences, *i.e.*, much slower than 205 s^{-1}.

The $^{13}C^\gamma$ chemical shifts of the different aromatic amino-acid types (phenylalanine and tyrosine) are well separated. However, the $^{13}C^\gamma$ resonances within one amino-acid type seem to be less disperse than their $^{13}C^\beta$ counterparts. All phenylalanine and tyrosine $^{13}C^\beta$'s of cutinase fall into a region of 7.2 ppm, whereas the $^{13}C^\gamma$'s cover a region of 3.3 ppm, excluding the empty part of the spectrum between the two residue types. However, considering the threefold larger linewidth of the $^{13}C^\beta$ resonances compared to the $^{13}C^\gamma$ peaks, the $^{13}C^\gamma$ seems to be a better nucleus to correlate the aromatic proton chemical shifts with than the $^{13}C^\beta$, which is used for this purpose in the experiments proposed by Yamazaki *et al.* (*11*) and related pulse sequences (*12–14*).

Two factors will negatively affect the sensitivity of our experiments in comparison to the experiments of Yamazaki *et al.* (*11*): (i) The fourfold lower gyromagnetic ratio of ^{13}C relatively to ^1H and (ii) the longer longitudinal relaxation time (T_1) of $^{13}C^\gamma$ compared to the T_1 of $^1H^\beta$, requiring longer prescan recovery delays (T_{ps}). The latter point turned out not to be a limiting factor for the efficiency of the experiments described in this article, as we established that the T_{ps} yielding the maximal signal-to-noise ratio (S/N) per unit of acquisition time is only 1.5 s. The S/N per unit of acquisition time can be approximated as (neglecting the time of the experiment and acquisition)

$$S/N \sim I_\infty[1 - \exp(-T_{ps}/T_1)]/(T_{ps})^{-1/2}, \qquad [1]$$

where I_∞ is the signal intensity at infinite T_{ps}. This function has its maximum at $T_{ps} = 1.26 \cdot T_1$. Using the empirically determined optimal T_{ps} of 1.5 s, the T_1 of the $^{13}C^\gamma$ of aromatic residues is estimated to be 1.2 s.

In order to compare the two approaches, we performed 1D versions of the (Hβ)Cβ(CγCδ)Hδ experiment and our CG(CD)H experiment. The (HβCβCγCδ)Hδ was recorded with 1600 scans and a prescan recovery delay of 1 s, and the (CGCD)H with 1024 scans and a prescan delay of 1.5 s, so that they have comparable total acquisition times. The

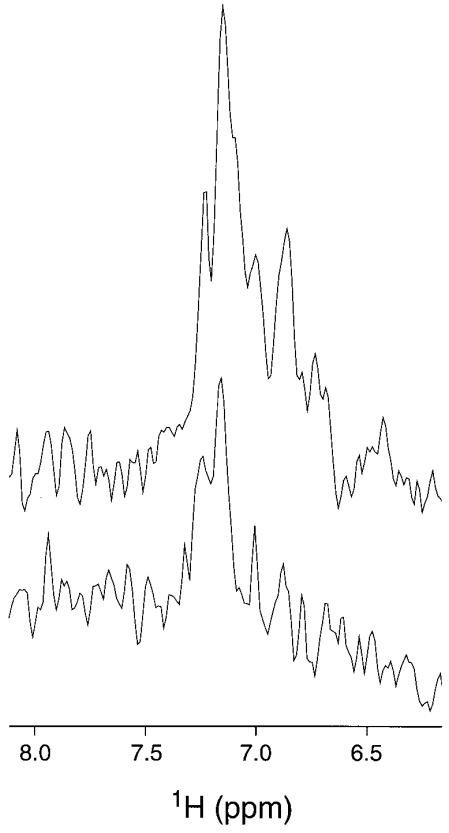

FIG. 3. One-dimensional (HβCβCγCδ)Hδ (lower trace) and (CGCD)H (upper trace) spectra of cutinase recorded with comparable total acquisition times.

results are shown in Fig. 3. The S/N of the (CGCD)H is about two times higher than the S/N of the (HβCβCγCδ)Hδ. Apparently, the loss in sensitivity due to the lower gyromagnetic ratio and the slightly longer T_1 of $^{13}C^\gamma$ compared to those of $^1H^\beta$ is compensated for by the fact that losses due to relaxation and B_1 inhomogeneity during the pulses are smaller in the shorter pulse sequence. As the CG(CD)H yields a S/N two times higher than that of the (Hβ)Cβ(CγCδ)Hδ and as the CG(CB)H is not only used in combination with the CG(CD)H, but also with the CG(CDCE)H, CG(CDCECZ)H, and CG(C^{aro})H-TOCSY experiments, the suite of experiments we propose will at least be equally efficient on a per unit acquisition-time basis when compared to the experiments of Yamazaki *et al.* (*11*).

The sensitivity of the CG(CD)H, CG(CDCE)H, and CG(CDCECZ)H experiments decreases progressively, due to B_1 inhomogeneity during the pulses and due to relaxation during the transfer step that is added to each successive experiment. For each extra transfer step, the S/N drops by a factor of three, leaving hardly any signals above the noise level in the CG(CDCECZ)H experiment. Comparing the performance of the relay-type and the TOCSY experiments, the CG(CD)H appears to be the most sensitive experiment

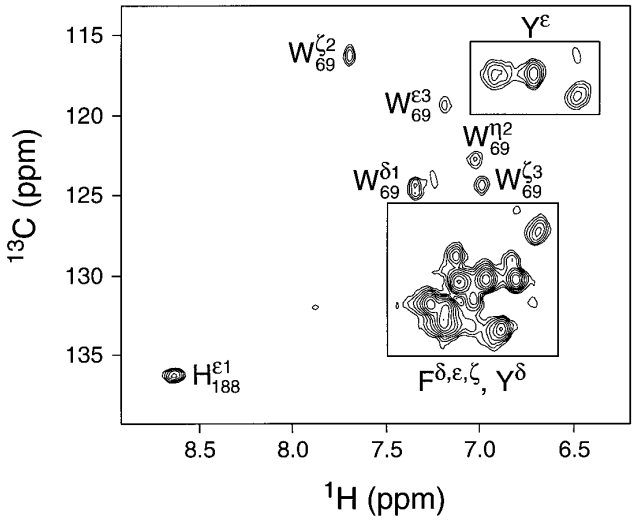

FIG. 4. Two-dimensional $^{13}C-^{1}H$ semi-constant-time COSY spectrum of uniformly ^{13}C, ^{15}N-labeled cutinase recorded with parameters optimized for the aromatic resonances.

to correlate the δ protons. For reaching the ϵ protons, the CG(CD)H and CG(C^{aro})H–TOCSY experiments perform equally well. For the phenylalanine residues, the ζ protons could only be reached with good sensitivity by means of the TOCSY experiment (see Fig. 2A).

Figure 4 shows a 2D $^{13}C-^{1}H$ semi-constant-time COSY spectrum, recorded with parameters optimized for the aromatic resonances (*18, 28*). The δ, ϵ, and ζ correlations of the phenylalanines and the δ correlations of the tyrosines are highly overlapping. Also the ϵ correlations of the tyrosines, which appear more upfield in the ^{13}C dimension, have nearly overlapping signals. The aromatic resonances could therefore not be assigned from the 3D CCH– and H(C)CH–TOCSY experiments, which were recorded with parameters optimized for the aromatic resonances (*28*). Having assigned the aromatic proton frequencies from the experiments presented in this article, only a few $^{13}C^{\delta}$, $^{13}C^{\epsilon}$, and $^{13}C^{\zeta}$ chemical shifts could be obtained from the SCT-COSY spectrum. Their degeneracy will likewise hamper the interpretation of the aromatic region of a ^{13}C-edited NOESY.

The CG(CB)H and CG(CD)H can also be applied to histidine residues by optimizing them for the more upfield-shifted $^{13}C^{\beta}$ and $^{13}C^{\delta 2}$ resonances compared to those of phenylalanines and tyrosines. Cutinase contains only one histidine, the active site His^{188}. Its $^{13}C^{\epsilon 1}$, $^{1}H^{\epsilon 1}$ correlation was readily recognized in the $^{13}C-^{1}H$ SCT-COSY spectrum by its characteristic ^{13}C and ^{1}H shifts (see Fig. 4). The $^{1}H^{\delta 2}$ frequency of His^{188} was determined from NOEs in ^{15}N- and ^{13}C-edited NOESY spectra. However, this correlation was not observed in the $^{13}C-^{1}H$ SCT-COSY spectrum (*28*).

In the same manner the CG(CB)H and CG(CD)H can be applied to tryptophan residues by optimizing them for the more upfield-shifted $^{13}C^{\beta}$ and $^{13}C^{\gamma}$ chemical shifts compared to those of phenylalanines and tyrosines. Cutinase contains only one tryptophan, Trp^{69}. For this residue, all aromatic carbon and carbon-bound proton frequencies could be assigned from the CCH–TOCSY experiment (*28*), because of their better dispersion in comparison to the phenylalanine and tyrosine signals (see Fig. 4). The $^{13}C^{\delta 1}$, $^{1}H^{\delta 1}$ pair served as the starting point. This correlation was easily recognized in a $^{13}C-^{1}H$ CT-COSY spectrum with a carbon evolution period tuned to $1/^{1}J_{CC}$ (*18*), where it was the only peak with an opposite sign relative to the other peaks from most aromatic carbons, having an even number of carbon neighbors.

In this article we have presented four 2D experiments for correlating the $^{13}C^{\gamma}$ and aromatic proton chemical shifts of aromatic residues. Another experiment which correlates the $^{13}C^{\gamma}$ and $^{1}H^{\beta}$ chemical shifts unambiguously links the aromatic proton assignments to the aliphatic portion of the residue. Because of the relatively short coherence transfer pathways, the experiments are applicable for proteins with a molecular weight larger than 20 kDa. The experiments are easily extended to 3D versions, in which the other aromatic carbon or $^{13}C^{\beta}$ chemical shifts are recorded as well. They provide a simple approach for the unambiguous sequence-specific assignment of aromatic side chains.

ACKNOWLEDGMENTS

J.J.P. was supported by a grant from Unilever Research. We thank A. J. Fellinger, M. C. D. van der Burg-Koorevaar, J. E. M. van Nieuwenhoven, P. Ravestein, and A. J. van de Wijngaard for the production and purification of the uniformly ^{13}C, ^{15}N-labeled sample of cutinase, E. Ulrich for extracting aromatic $^{13}C^{\gamma}$ chemical shifts from the BioMagResBank, and R. H. A. Folmer for carefully reading the manuscript.

REFERENCES

1. A. Bax and S. Grzesiek, *Acc. Chem. Res.* **26,** 131–138 (1993).
2. A. S. Edison, F. Abildgaard, W. M. Westler, E. S. Mooberry, and J. L. Markley, *Methods Enzymol.* **239,** 3–79 (1994).
3. K. Wüthrich, ''NMR of Proteins and Nucleic Acids,'' Wiley, New York (1986).
4. T. Yamazaki, M. Yoshida, and K. Nagayama, *Biochemistry* **32,** 5656–5669 (1993).
5. G. W. Vuister, S.-J. Kim, C. Wu, and A. Bax, *J. Am. Chem. Soc.* **116,** 9206–9210 (1994).
6. L. E. Kay, M. Ikura, and A. Bax, *J. Am. Chem. Soc.* **112,** 888–889 (1990).
7. A. Bax, G. M. Clore, P. C. Driscoll, A. M. Gronenborn, M. Ikura, and L. E. Kay, *J. Magn. Reson.* **87,** 620–627 (1990).
8. O. Zerbe, T. Szyperski, M. Ottiger, and K. Wüthrich, *J. Biomol. NMR* **7,** 99–106 (1996).
9. S. W. Fesik, H. L. Eaton, E. T. Olejniczak, E. R. P. Zuiderweg, L. P. McIntosh, and F. W. Dahlquist, *J. Am. Chem. Soc.* **112,** 886–888 (1990).
10. A. Bax, G. M. Clore, and A. M. Gronenborn, *J. Magn. Reson.* **88,** 425–431 (1990).

11. T. Yamazaki, J. D. Forman-Kay, and L. E. Kay, *J. Am. Chem. Soc.* **115,** 11,054–11,055 (1993).

12. S. Grzesiek and A. Bax, *J. Am. Chem. Soc.* **117,** 6527–6531 (1995).

13. T. Carlomagno, M. Maurer, M. Sattler, M. G. Schwendinger, S. J. Glaser, and C. Griesinger, *J. Biomol. NMR* **8,** 161–170 (1996).

14. F. Löhr and H. Rüterjans, *J. Magn. Reson. B* **112,** 259–268 (1996).

15. B. R. Seavey, E. A. Farr, W. M. Westler, and J. L. Markley, *J. Biomol. NMR* **1,** 217–236 (1991).

16. R. Powers, A. M. Gronenborn, G. M. Clore, and A. Bax, *J. Magn. Reson.* **94,** 209–213 (1991).

17. K. Dijkstra, G. J. A. Kroon, N. A. J. van Nuland, and R. M. Scheek, *J. Magn. Reson. A* **107,** 102–105 (1994).

18. G. W. Vuister and A. Bax, *J. Magn. Reson.* **98,** 428–435 (1992).

19. M. A. McCoy and L. Mueller, *J. Magn. Reson.* **99,** 18–36 (1992).

20. A. Bax and S. S. Pochapsky, *J. Magn. Reson.* **99,** 638–643 (1992).

21. E. T. Olejniczak and S. W. Fesik, *J. Am. Chem. Soc.* **116,** 2215–2216 (1994).

22. B. A. Messerle, G. Wider, G. Otting, C. Weber, and K. Wüthrich, *J. Magn. Reson.* **85,** 608–613 (1989).

23. L. E. Kay, M. Ikura, R. Tschudin, and A. Bax, *J. Magn. Reson.* **89,** 496–514 (1990).

24. A. J. Shaka, J. Keeler, T. Frenkiel, and R. Freeman, *J. Magn. Reson.* **52,** 335–338 (1983).

25. A. J. Shaka, P. B. Barker, and R. Freeman, *J. Magn. Reson.* **64,** 547–552 (1985).

26. A. Mohebbi and A. J. Shaka, *Chem. Phys. Lett.* **178,** 374–378 (1991).

27. D. Marion, M. Ikura, R. Tschudin, and A. Bax, *J. Magn. Reson.* **85,** 393–399 (1989).

28. J. J. Prompers, A. Groenewegen, R. C. van Schaik, H. A. M. Pepermans, and C. W. Hilbers, *Protein Sci.* **6,** 2375–2384 (1997).

29. G. Zhu and A. Bax, *J. Magn. Reson.* **90,** 405–410 (1990).